New Journal of Physics
The open-access journal for physics

Designing plasmas for chronic wound disinfection

T Nosenko[1,2,3], T Shimizu[1] and G E Morfill[1]

[1] Max-Planck Institute for Extraterrestrial Physics, Garching, Germany
[2] Institute of Pathology, Technical University of Munich, Munich, Germany
E-mail: tnosenko@mpe.mpg.de

New Journal of Physics **11** (2009) 115013 (19pp)
Received 6 March 2009
Published 26 November 2009
Online at http://www.njp.org/
doi:10.1088/1367-2630/11/11/115013

Abstract. Irradiation with low-temperature atmospheric-pressure plasma provides a promising method for chronic wound disinfection. To be efficient for this purpose, plasma should meet the following criteria: it should significantly reduce bacterial density in the wounded area, cause a long-term post-irradiation inhibition of bacterial growth, yet without causing any negative effect on human cells. In order to design plasmas that would satisfy these requirements, we assessed the relative contribution of different components with respect to bactericidal properties due to irradiation with argon plasma. We demonstrate that plasma-generated UV radiation is the main short-term sterilizing factor of argon plasma. On the other hand, plasma-generated reactive nitrogen species (RNS) and reactive oxygen species (ROS) cause a long-term 'after-irradiation' inhibition of bacterial growth and, therefore, are important for preventing wound recolonization with bacteria between two treatments. We also demonstrate that at certain concentrations plasma-generated RNS and ROS cause significant reduction of bacterial density, but have no adverse effect on human skin cells. Possible mechanisms of the different effects of plasma-generated reactive species on bacteria and human cells are discussed. The results of this study suggest that argon plasma for therapeutic purposes should be optimized in the direction of reducing the intensity of plasma-generated UV radiation and increasing the density of non-UV plasma products.

[3] Author to whom any correspondence should be addressed.

Contents

1. Introduction

Plasma medicine is one of the most recent developments, which has emerged at the boundary of plasma physics, chemistry and biomedical sciences [1, 2]. The leading idea of plasma medicine is to employ low-temperature atmospheric-pressure plasmas for generating biologically active agents and their delivery to selected loci of the human body for therapeutic purposes. These active agents include charged particles, metastable-state molecules or atoms, reactive species (RS: free radicals and some ground state molecules such as ozone and peroxides), and ultraviolet (UV) radiation. Understanding the processes induced by the interaction of these components with gases and liquids and the effects of the reaction products on living cells is a prerequisite for defining potential areas of plasma application in medicine and to designing purpose-specific plasmas. In doing this one can treat plasmas like a medical cocktail, which contains new and established agents that can be applied at the molecular (atomic, ionic) level to cells in prescribed intensities and overall doses.

One feature of plasmas that potentially can be employed for therapeutic purposes is their bactericidal properties [3]–[5]. Bactericidal properties of plasmas have been intensively studied and utilized for the decontamination and sterilization of air-exposed surfaces (medical instruments, catheters, packages, containers and premises [6, 7]). High sterilization efficacy of plasmas is achieved by synergy of different plasma components. This feature can be used in particular for the chronic wound disinfection as an addition or even alternative to antibiotic therapy, in particular where antibiotic resistant bacteria are encountered. To be efficient in chronic wound disinfection, plasmas should meet the following criteria: (i) they should significantly reduce bacterial density in the wounded area, (ii) cause a long-term post-irradiation inhibition of bacterial growth, and (iii) have no negative effect on human cells. Designing plasmas that would satisfy these criteria is a challenging task. The bactericidal effect of plasma irradiation greatly relies on mutagenic and oxidative properties of plasma-generated UV radiation and RS. While toxic for bacteria, these plasma components would also

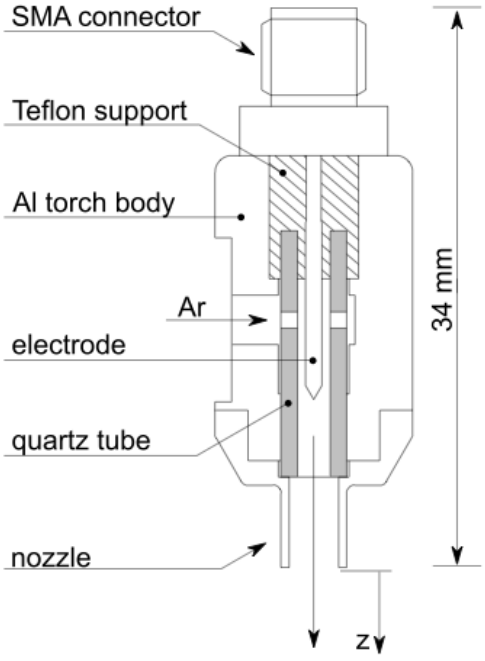

Figure 1. Schematic representation of the plasma torch system.

affect human cells and tissues in a dosage-dependent manner [8]–[11]. Therefore, it is critical to identify plasma components that have differential effects on bacteria and mammalian cells (specifically, cells relevant to wounds) and define their dosage thresholds.

The aim of the present study is to assess the relative bactericidal contribution of different plasma components, both separately and in combination. Our ultimate goal is to identify plasma components (or products of their reactions) that would have different effects on bacteria and human cells. The data obtained in this study provide a basis for designing plasmas for wound disinfection.

2. Experimental apparatus and plasma irradiation conditions

The plasma torch consists of a 34 mm long aluminum cylinder, a quartz glass tube and a titanium-powered electrode (1 mm in diameter) with a sharpened tip (see figure 1). The powered electrode is placed coaxially in the quartz tube covered by the aluminum cylinder. The feed gas is chilled in the dry-ice cooling system and flows from the middle of the torch along the electrode to the nozzle. Microwave plasma is produced between the tip of the powered electrode and the surface of the quartz tube. The microwave power at 2.45 GHz is transferred through a coaxial cable via a small 3-stub tuner from the microwave generator. The aluminum cylinder is electrically grounded through the coaxial cable and the microwave generator. The microwave plasma flows with the feed gas from the nozzle of the torch (2 mm in diameter).

In this study, the torch was positioned with the principal axis perpendicular to the ground. The feed gas, argon (99.998% purity), was supplied at a flow rate of 140 or 700 sccm. The microwave power was 2 W. These values of the gas flow and microwave power have been established as the minimal values required to generate a stable plasma efficient in sterilizing the surface of solid agar media inoculated with *Escherichia coli*.

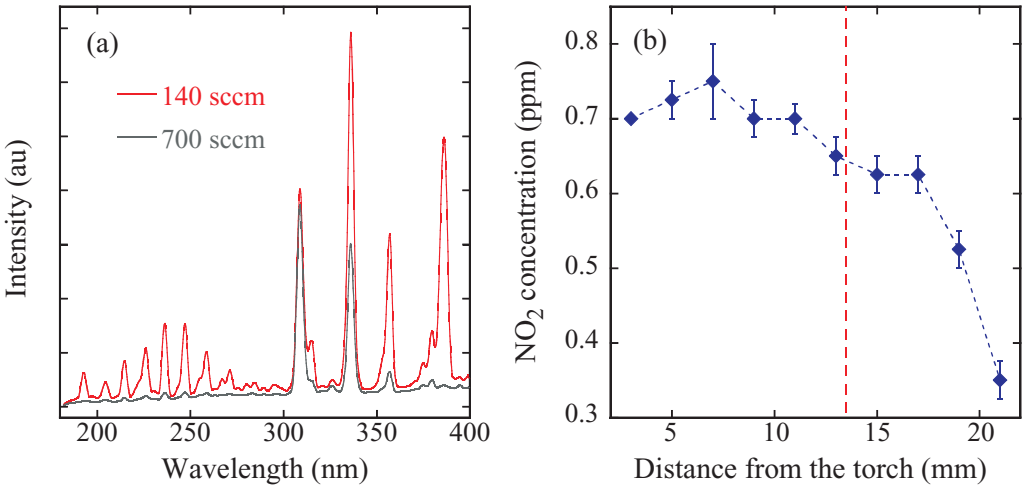

Figure 2. Optical emission spectra in the UV range (a) and concentration of reactive nitrogen species (RNS) (b) produced by the plasma torch system. Optical emission spectra in the UV range were measured at Ar flow rates of 140 and 700 sccm. Concentration of NO_2 was measured at microwave power of 2 W and Ar flow rate of 140 sccm.

Bacterial suspensions and liquid samples used for the analysis of hydrogen peroxide (H_2O_2) and nitrite/nitrate concentration were irradiated in 96-microwell plates (Nunc; 167008) in a volume of 70 μl well^{-1}. Samples of media and phosphate buffered saline (PBS) for the human skin fibroblast viability and migration assays were irradiated in 12-well plates (Greiner; 665180) in a volume of 1000 μl well^{-1} for 60 min ($\sim$ 5 min/70 μl). To achieve an even distribution of plasma across the sample surface, test plates were irradiated on a rotating positional table. The rotation amplitude and speed were adjusted depending on the well/plate diameter. In all experiments, the distance from the plasma torch to the liquid surface (z) was 13.5 mm (16 mm to the bottom of the test plate). To assess the effects of plasma-generated UV radiation, samples were irradiated through a quartz glass placed on top of the test plate (see figure A.1 for the spectral transmission characteristics of the quartz glass). The detailed description of the experimental methods used in this study is provided in the appendix.

UV radiation produced by argon plasma under the given conditions was polychromatic with four main peaks at 309, 336, 357 and 386 nm (see figure 2(a)). The difference between the optical emission spectra produced by the torch at different Ar flow rates reflects the ambient air interaction with the argon plasma in our experiments. UV power ($\lambda = 170$–340 nm) at the liquid surface was 11.4 μW cm^{-2}. The concentration of nitrogen dioxide (NO_2) at this position was $\sim$ 0.650 ppm (see figure 2(b)). The pH of PBS and deionized water did not change due to plasma irradiation; pH of the organic solutions, Luria broth (LB) medium and Dulbecco's modified Eagle medium (DMEM), increased by $\sim$ 0.5 after 10 min of plasma treatment. The temperature of liquids irradiated with plasma at $z = 13.5$ mm did not exceed 30 °C ($\Delta T = 2 \pm 0.25$ °C after 5 min of plasma irradiation, see figure 3(a)). Evaporation from the liquid surface in 96- and 12-well plates was 3 and 7 μl min^{-1}, respectively (see figure 3(b)). To compensate for the evaporation, we added corresponding volumes of deionized water to the samples during plasma irradiation.

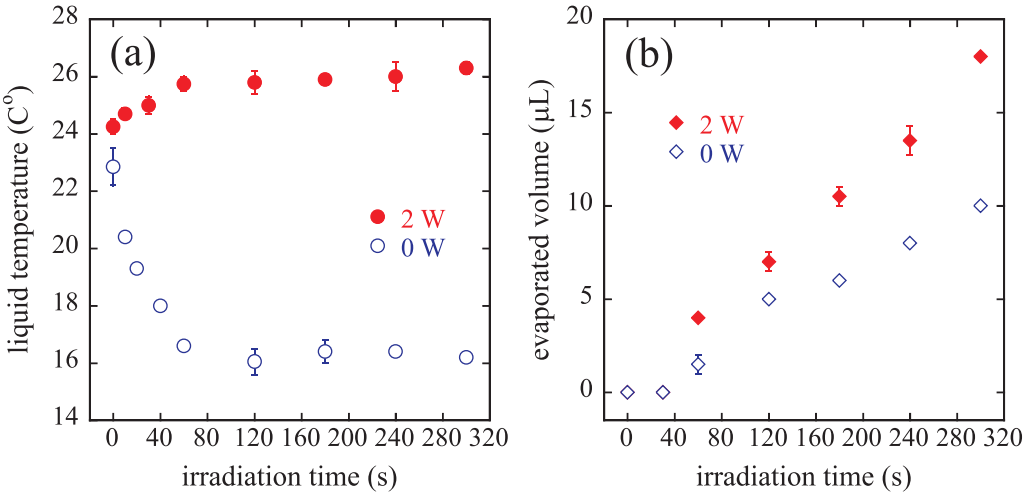

Figure 3. Temperature (a) and evaporation (b) of liquids irradiated with argon plasma. Plasma was generated at microwave power of 2 W and Ar flow rate of 140 sccm. Samples of deionized water were plasma-irradiated in 96-well plates (70 μl well^{-1}) at $z = 13.5$ mm. Control samples were treated with Ar without plasma (0 W).

3. Results and discussion

3.1. Effect of plasma and plasma-generated UV on the density of bacteria submerged in liquids

Reduction of bacterial density on the air-exposed surface of solid agar media after irradiation with argon plasma has been reported previously [4, 12]. However, in wounds bacteria are typically submerged in various liquids, including blood, wound fluid and saline solution that is frequently used for wound irrigation and their pretreatment for the antibacterial therapy [13]. Therefore, our experiments were designed to test the effects of plasma irradiation on bacteria submerged in liquids. Two different types of liquids were used in this study: PBS and LB bacterial growth medium. PBS is an inorganic solution, in which bacteria remain viable for a relatively long time, but do not reproduce. On the other hand, LB medium provides all components necessary to support viability and high reproductive activity of *E. coli*. The two liquids differ in their physical characteristics as well. According to our measurements (see appendix A.1), a 2.5 mm column of LB absorbs 97% of plasma-generated UV radiation at $\lambda = 170$–340 nm. The same column of PBS absorbs less than 30% of the plasma-generated UV.

Analyses of *E. coli* samples plasma-irradiated in LB medium and PBS under conditions described in section 2 show that irradiation with argon plasma causes significant reduction of bacterial density in both types of liquids (see figure 4). There was a positive correlation between the bacterial density reduction and irradiation duration. However, the bactericidal efficacy of plasma irradiation strongly depends on the physical properties and chemical composition of liquids. Thus, the irradiation time required for the complete disinfection of 70 μl of PBS was five times shorter than the time required to achieve 100% bacterial density reduction in the LB medium. The lower effect of plasma on bacteria in the LB medium can be explained by the relative reduction of the UV contribution due to its absorption by the medium.

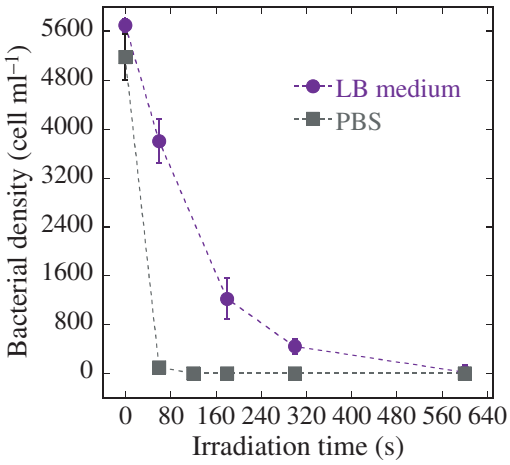

Figure 4. *E. coli* density in bacterial growth LB medium and PBS after plasma irradiation.

To estimate the bactericidal contribution of plasma-generated UV radiation, we compared the bacterial density reduction in *E. coli* samples in PBS and LB medium due to their treatment with plasma and with plasma-generated UV only (through a quartz glass; see figure 5). The results of this experiment demonstrate that UV radiation was the only sterilizing factor in PBS disinfection (see figure 5(a)). Bacterial density in samples irradiated with plasma did not differ significantly from the bacterial density in pure UV-treated samples. According to the results of previous experiments [12], plasma irradiation had significantly higher efficacy in sterilization of air-exposed surfaces than plasma-generated UV only. The difference between the results of the two experiments suggests that liquids screen bacteria from the plasma-generated RS and charged particles. However, the contribution of non-UV plasma components to the liquid sterilization becomes evident in samples irradiated in LB medium for 5–10 min (see figure 5(b)). The overall bactericidal efficacy of the plasma was approximately two times higher than the bactericidal efficacy of plasma-generated UV only. In these samples, the UV contribution was limited by low transparency of the LB medium.

Bactericidal efficacy of plasma and UV irradiation depends also on the initial bacterial density in irradiated samples. This 'loading effect' has been described previously for the plasma sterilization of solid surfaces [14, 15]. The observed correlation between the initial bacterial density and the efficacy of surface sterilization was nonlinear and differed for plasma and UV radiation. We observed similar trends in our experiments, in which an LB medium containing different densities of *E. coli* was irradiated with either plasma or plasma-generated UV only (see figure 6). In addition, the results of this experiment show that the relative bactericidal contribution of the plasma-generated UV and 'non-UV' plasma components also depends on the initial bacterial density in the liquid medium. There are several factors that explain the observed correlation including (i) the geometry of bacterial distribution in the irradiated liquids (shadowing by bacteria [15] and shadowing by the medium) and (ii) buffering (antioxidative) activity of the bacterial suspension. The geometry of bacterial distribution has the major effect on the sterilizing efficacy of UV radiation. The antioxidative potential of the bacterial samples, which depends on the bacterial density, determines the level of sensitivity to different concentrations of plasma-generated RS.

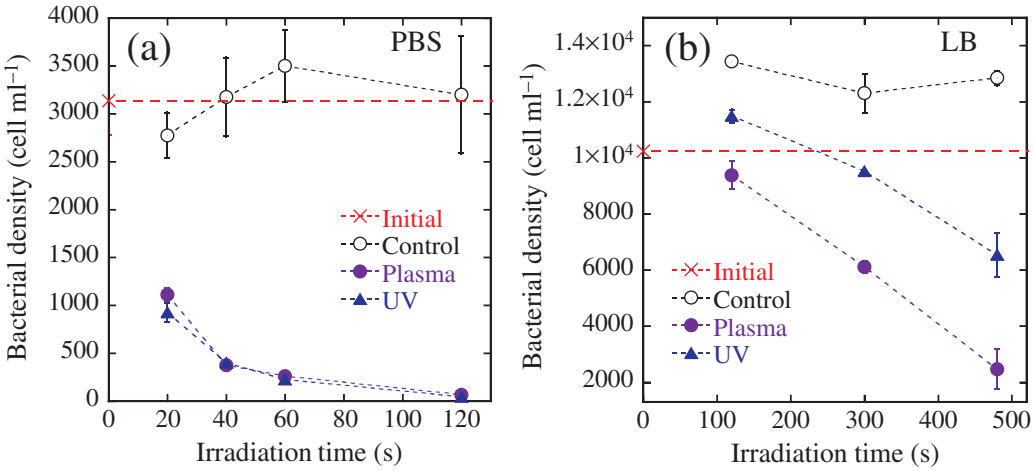

Figure 5. Effects of irradiation with plasma and plasma-generated UV radiation only on the *E. coli* density in PBS (a) and LB medium (b). Bacterial density in plasma- and UV-irradiated samples and untreated control samples was assayed after 60 min of incubation at room temperature. The red dashed line indicates the initial density of *E. coli* in all samples before their irradiation and incubation.

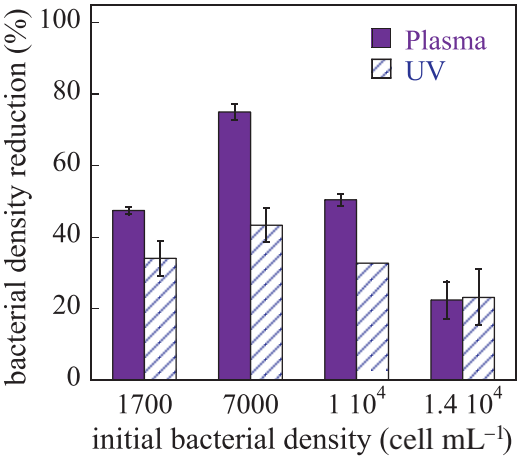

Figure 6. Correlation between the initial bacterial density and the rate of bacterial density reduction after plasma and UV irradiation. *E. coli* suspensions in LB medium (70 μl sample^{-1}) of different densities were irradiated with plasma or with plasma-generated UV radiation for only 5 min. Bacterial density in treated samples was assayed after 60 min of incubation at room temperature.

3.2. After-irradiation dynamics of bacterial density in LB medium

In most of our experiments, a small fraction of bacteria survived a single plasma treatment in liquid media (see figure 5(b)) and on air-exposed surfaces [4, 12]. Population duplication time (generation time) for most known bacteria ranges from 15 min to 1 h. For example, generation time of a methicillin-resistant *Staphylococcus aureus*, one of the most frequent and problematic pathogens of chronic wounds, is 24–30 min [16]. Due to the short generation time, bacteria

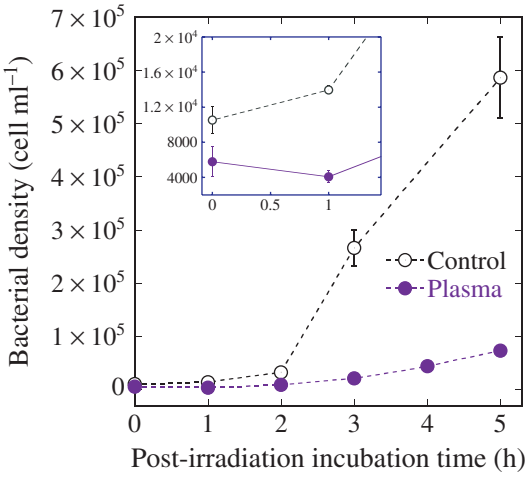

Figure 7. Dynamics of bacterial density in LB medium after plasma irradiation. *E. coli* suspension in LB medium (70 μl sample^{-1}) was plasma-irradiated for 5 min and incubated at 37 °C. Control samples were prepared identically, but not irradiated. Bacterial density in treated and control samples was assayed for 5 h after plasma irradiation.

can rapidly recolonize the treatment area. To prevent bacterial recolonization of the wound between two treatments, a successful antibacterial therapy should cause a long-term inhibition of bacterial growth.

To assess the dynamics of bacterial density after plasma irradiation, we treated *E. coli* samples in LB medium with plasma (5 min sample^{-1}) and assayed bacterial density in treated and control samples for 5 h after the treatment. The results of this experiment are presented in figure 7. Bacterial density declines during the first hour after the treatment (see inset in figure 7) and then gradually grows during the next 4 h of the experiment. The comparison of treated and control samples reveals significant inhibition of bacterial growth in plasma-irradiated samples. Three and 5 h after the treatment, the bacterial density in plasma-irradiated samples was only 8% and 12% of the bacterial density in control samples, respectively.

3.3. Effect of plasma- and UV-irradiated liquids on bacterial viability and reproduction

Experimental results presented in sections 3.1 and 3.2 suggest that plasma-irradiated LB medium possesses bactericidal properties. To verify whether the observed trend is LB-specific, caused by interactions of plasma-generated RS with organic compounds of the medium, we tested the effects of plasma- and UV-irradiated PBS and LB medium on the viability and reproduction of non-irradiated *E. coli*. As shown in figure 8, significant reduction of bacterial density (in comparison with control samples) was observed in both inorganic and organic solutions when they were plasma-irradiated for at least 5 min. This fact is evidence that the toxicity of plasma-irradiated liquids for bacteria is independent of their chemical composition. There are two possible mechanisms that contribute to the reduction of bacterial density in plasma-irradiated LB medium: (i) cell mortality and (ii) inhibition of bacterial reproduction by plasma products. Since bacteria do not reproduce in PBS, cell mortality is the only mechanism of bacterial density reduction in plasma-irradiated PBS. Incubation in liquids irradiated with

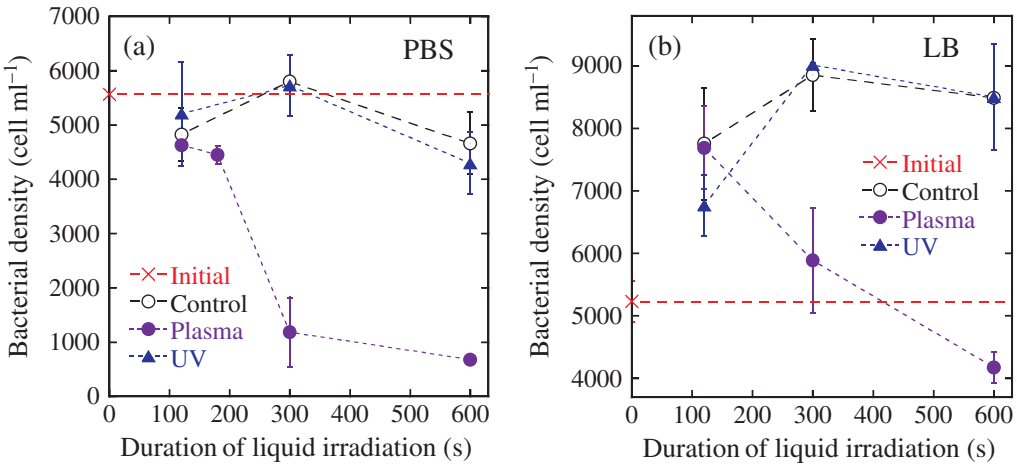

Figure 8. Effects of plasma-irradiated PBS (a) and LB medium (b) on density of non-irradiated *E. coli*. Ten microliters of non-irradiated *E. coli* suspension were mixed with 60 μl of plasma- or UV-irradiated liquids immediately after the irradiation. Control samples were prepared in non-irradiated liquids. Bacterial density in treated and control samples was assayed after 60 min incubation at room temperature. The red dashed line indicates the initial bacterial density in all samples before the irradiation and incubation.

plasma-generated UV did not have any detectable effect on *E. coli* (see figure 8). This result confirms that airborne plasma components that have diffused into the liquids play an important role in the observed post-irradiation inhibition of bacterial growth. Note that the irradiation time required for the accumulation of plasma-generated molecules (RS and products of their reactions) at the concentrations toxic for bacteria (at given bacterial densities) was about two times longer than the time required for the complete sterilization of PBS by plasma-generated UV (see figures 5(a) and 8).

The shape of the post-irradiation bacterial density curve (see figure 7) suggests that plasma-irradiated liquids have stronger bactericidal properties during the first hour after the irradiation. The results of our experiment presented in figure 9 provide additional support for this conclusion. In this experiment, the bacterial density was 9.6% and 10.8% lower in samples treated with plasma-irradiated PBS and LB medium, respectively, immediately after irradiation than in samples treated with the same liquids after a 60 min delay.

3.4. Plasma-generated reactive nitrogen species (RNS) and reactive oxygen species (ROS)

Bactericidal properties of the plasma irradiated liquids can be attributed to the RS generated in the gas and liquid phases during plasma irradiation, such as nitric oxide (NO), NO_2, superoxide (O_2^-), hydroxide (HO^-), H_2O_2, etc. In our experiments, the concentration of NO_2 in the gas phase at the liquid surface was 0.65 ppm (see figure 2(b)). Even though the coefficients of NO and NO_2 diffusion and solubility in water and PBS are known [17, 18], we were not able to calculate the concentrations of these species in plasma-irradiated liquids due to the convection caused by the Ar flow.

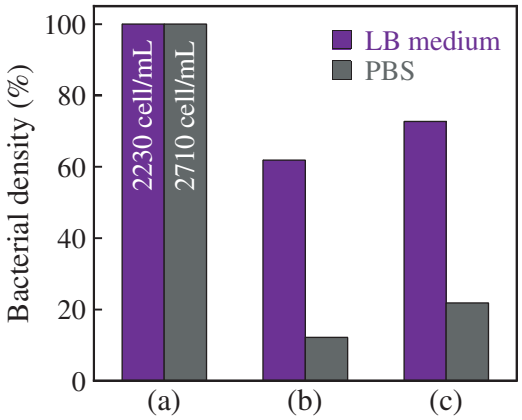

Figure 9. Post-irradiation decline in bactericidal efficacy of plasma-irradiated liquids. Sixty microliters of LB medium and PBS were plasma-irradiated for 10 min. Ten microliters of non-irradiated suspension of *E. coli* were mixed with plasma-irradiated liquids either immediately (b) or 60 min after the irradiation (c). Bacterial density in plasma-irradiated liquids was assayed after 60 min of incubation at room temperature. The initial bacterial density in non-irradiated liquids (a) was measured before the incubation.

In aqueous solutions and biological fluids, nitric oxide and nitrogen dioxide undergo a series of reactions including:

$$NO + O_2^- \rightarrow ONO_2^- + H^+ \rightarrow NO_3^- + H^+,$$

$$NO + O_2 \rightarrow N_2O_3^- + H_2O \rightarrow NO_2^- + NO_3^-,$$

$$NO + NO_2 \rightarrow N_2O_3 + H_2O \rightarrow 2NO_2^-.$$

End products of these reactions are nitrites and nitrates. In this study, we used the concentrations of nitrites and nitrates as a measure of RNS concentration in plasma-irradiated liquids. Results of our measurements show that irradiation with argon plasma under the given parameters produced physiological (micromolar) concentrations of nitrites and nitrates in PBS and LB medium (see figure 10). Nitrite concentration in plasma-irradiated liquids was extremely unstable. It depended on the chemical composition of the irradiated liquids, concentration of dissolved oxygen, and time passed after the irradiation (see figures 10 and 11). The total concentration of plasma-generated nitrites and nitrates proved to be a more reliable measure. There was a positive correlation between the nitrite/nitrate concentration and duration of plasma irradiation and, consequently, bacterial density reduction in plasma-irradiated liquids.

A positive correlation was also observed between the duration of plasma irradiation and concentration of H_2O_2 in plasma-irradiated PBS (see figure 12). There are several possible sources of H_2O_2 in plasma-irradiated aqueous solutions including diffusion of plasma-generated ROS from the gas phase, photolysis of water molecules by UV radiation and, possibly, hydrolysis by charged particles and metastable Ar atoms. The comparison of H_2O_2 concentrations in PBS, irradiated with the plasma and plasma-generated UV radiation only, showed that under the given experimental conditions UV-induced photolysis of water was the main factor of H_2O_2 generation (see figure 12) according to the following reaction:

$$\dot{O}H + \dot{O}H \rightarrow H_2O_2.$$

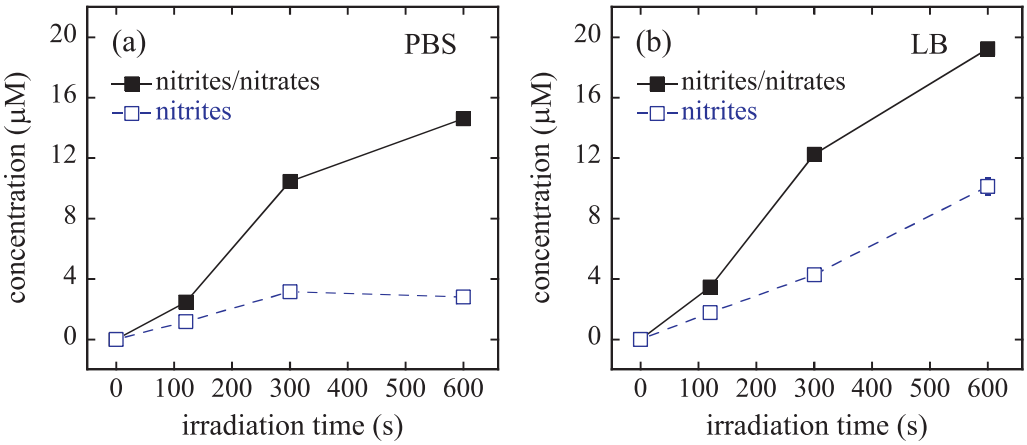

Figure 10. Concentrations of nitrites and nitrates in plasma-irradiated PBS (a) and LB medium (b). Nitrite and nitrate concentrations were measured in samples of PBS and LB medium prepared in the experiment presented in figure 8.

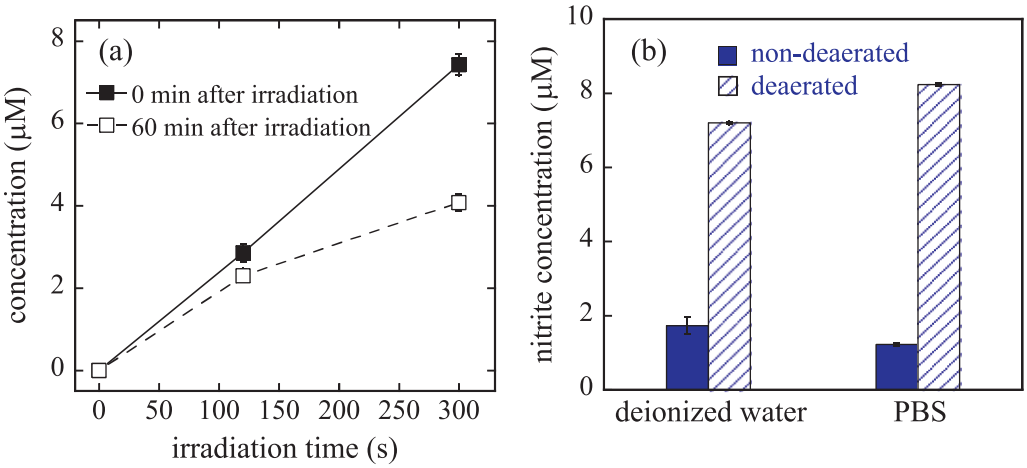

Figure 11. Instability of nitrite concentration in plasma-irradiated liquids. (a) Post-irradiation decay of nitrite concentration in plasma-irradiated liquids. Nitrite concentrations were measured in the samples of deionized water either immediately or 60 min after plasma irradiation. (b) Correlation between nitrite concentration and dissolved oxygen level in plasma-irradiated liquids. Nitrite concentrations were measured in the samples of deaerated and non-treated deionized water and PBS immediately after plasma irradiation.

Under modified experimental parameters, particularly increased gas flow rate, we also observed a UV-independent generation of H_2O_2 in plasma-irradiated aqueous solutions (data are not shown). Concentration of H_2O_2 in plasma- and UV-irradiated liquids was unstable. It changed during the first hour after the irradiation (see figure 13). Post-irradiation changes in the hydrogen peroxide and nitrite concentrations provide evidence that continuous reactions take place in liquids after the plasma irradiation. These reactions may provide an explanation for the observed decline of bactericidal properties of plasma-irradiated liquids during the first hour after the irradiation (see figure 9).

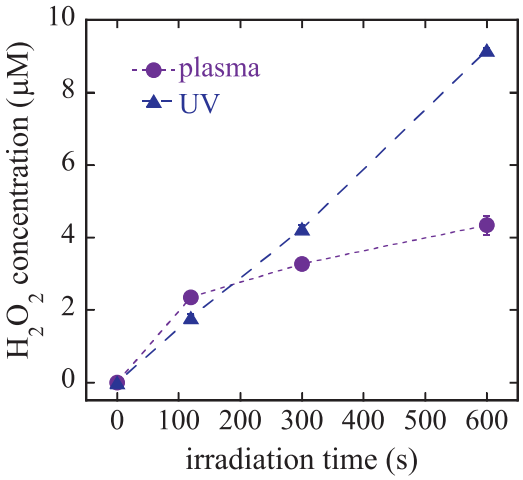

Figure 12. Concentration of H_2O_2 in PBS irradiated with plasma and plasma-generated UV radiation only. Concentrations of H_2O_2 were measured in PBS samples irradiated with plasma either directly or through the quartz glass. Relatively low concentration of H_2O_2 in samples irradiated with plasma-generated UV for 2 min should be attributed to the partial UV absorption by the quartz glass. Relatively low concentration of H_2O_2 in samples irradiated with plasma for 5–10 min can be explained by interactions of hydroxyl radicals and hydroxide with airborne plasma components and/or by their loss due to evaporation. The observed trends were consistent over three independent experiments.

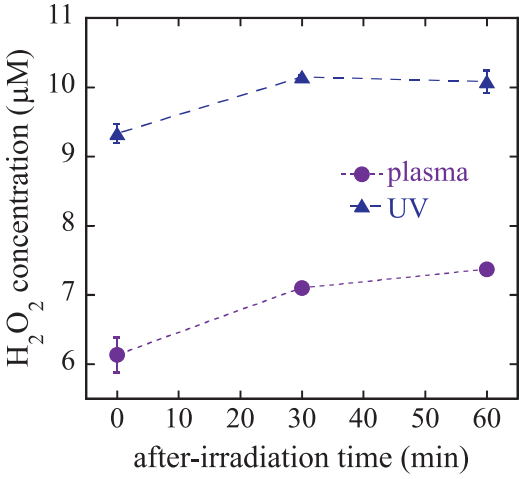

Figure 13. Post-irradiation alteration of H_2O_2 concentration in PBS treated with plasma and plasma-generated UV radiation only. PBS samples were irradiated with plasma either directly or through the quartz glass for 10 min. Concentrations of H_2O_2 in the samples were measured 0–60 min after the irradiation.

RNS and ROS are known to be highly toxic for bacteria. However, their toxic effect is dosage-dependent. Results of our experiments show that UV-generated H_2O_2 at concentrations 2–10 μM did not have any effect on *E. coli* density in PBS and LB medium (see figures 8 and 12). This observation is in agreement with previously published data [19, 20]. Imlay and Linn [19] detected a toxic effect of H_2O_2 on *E. coli* at the minimal concentration of 150 μM. We cannot explain the reduction of bacterial density in plasma-irradiated liquids solely by diffusion of nitric oxide from the gas phase either. Estimated concentrations of nitric oxide in liquids after 10 min of plasma irradiation in our experiments (see figure 10) were at least 10 times below its concentration toxic for bacteria [20, 21]. One possible explanation for the observed effect of plasma-irradiated liquids on bacteria is a synergy of ROS and RNS, particularly NO and H_2O_2. Nitric oxide is known to potentiate bacterial killing by low-concentration H_2O_2 [20, 22]. The mechanism of cooperative NO and H_2O_2 toxicity is not immediately obvious, because they do not react directly. A major portion of H_2O_2 cellular toxicity is attributed to DNA damage caused by derivatives of the iron-mediated Fenton reaction (hydroxyl radicals) [23]:

$$Fe^{2+} + H_2O_2 \rightarrow Fe^{3+} + OH^{\cdot} + OH^{-}.$$

Therefore the toxicity of H_2O_2 depends on the availability of intracellular iron ions. Under normal conditions, intracellular iron concentrations are kept low by iron-binding proteins. It was proposed that NO releases iron ions from intracellular metalloproteins and, by virtue of this, catalyses the reduction of H_2O_2 to the toxic $^{\cdot}$OH [20, 24]. Alternatively, NO diverts electron flow to free iron (Fe^{2+}) by blocking respiration in bacteria [22]. The cooperative action of non-toxic concentrations of NO and H_2O_2 is used by mammalian immune system cells, macrophages, to attack pathogenic micro-organisms. Even though activated macrophages produce a broad range of different RS [25], NO and H_2O_2 were demonstrated to be the major players of their cytotoxicity [20, 26].

3.5. Effect of plasma-irradiated liquids on viability and migration of human skin fibroblasts

The results of our experiments described in section 3.3 demonstrated that liquids acquire bactericidal properties after 5 min of plasma irradiation. To assess the relative effects of 'plasma liquids' on the human cell viability, we treated human skin fibroblast hTERT-Bj1 with PBS and DMEM irradiated with plasma at a similar rate. We did not detect any increase in the number of necrotic cells in cultures treated with plasma-irradiated liquids. Results of FACS analyses showed no apoptosis induction in hTERT-Bj1 cultures incubated in plasma-irradiated DMEM for 72 h (results are not shown here). Fibroblast migration rates in cultures incubated in plasma-irradiated and non-irradiated media did not differ significantly either (see figure 14). From image analyses, average migration rates were computed as 2.46 ± 0.17 and 2.59 ± 0.19 cells per hour per sector in treated and control samples, respectively.

We conclude that plasma-generated compounds at concentrations toxic for bacteria have no adverse effect on human skin fibroblast viability and migration. This conclusion again leads us to the idea that the observed bactericidal effect of 'plasma liquids' can be attributed to the synergy of plasma-generated nitric oxide and hydrogen peroxide. The differential effect of NO/H_2O_2 on bacteria and mammalian cells has been demonstrated previously. It has been shown that NO inhibits H_2O_2-induced apoptosis in several cell types including macrophages [27], fibroblasts, mesencephalic neurons [28], endothelial cells [29] and cardiomyoblasts [30] by inducing cellular synthesis of antioxidative enzymes. This cell response

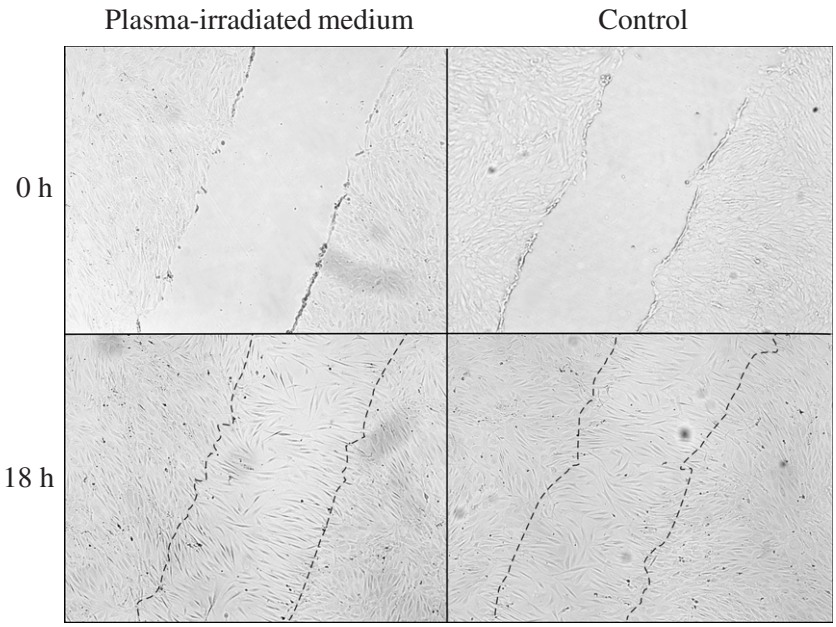

Figure 14. Human skin fibroblasts migration in the plasma-irradiated medium (scratch migration assay). hTETR-Bj1 in plasma-irradiated and non-irradiated DMEM/0.1% fetal calf serum (FCS) immediately (0 h) and 18 h after introducing the scratch. The dashed line indicates the initial scratch margins (at 0 h).

to low doses of NO has probably evolved as a protective mechanism against the macrophage cytotoxicity (see section 3.4).

We propose that plasma irradiation could potentially simulate the 'macrophage effect' and combat pathogenic bacteria by a combination of ROS and RNS. A more detailed study is required to assess effects of different concentrations of plasma-generated RS on different types of bacteria and human skin cells at different cell densities in order to identify optimal plasma composition and doses.

4. Conclusions

The results of this study demonstrate that:

1. Low-temperature atmospheric-pressure argon plasma is efficient for liquid sterilization.
2. Under the given experimental conditions, plasma-generated UV radiation represents the main short-term sterilizing factor of plasma irradiation.
3. Plasma-generated RNS and ROS cause a long-term post-irradiation inhibition of bacterial growth. This is important for preventing wound recolonization with pathogenic bacteria between two plasma treatments.
4. Concentrations of plasma-generated RS, which are toxic for bacteria but have no effect on human skin cells, can be achieved in practice.
5. Under the given experimental conditions, the irradiation time required for reaching concentrations of plasma-generated RS that are toxic for bacteria is about two times longer than the time required for the complete sterilization of transparent liquids by plasma-generated UV.

A major portion of the bactericidal effect of plasma-generated UV is attributed to the mutagenic properties of short-wavelength UV [31, 32]. Short-wavelength UV radiation is dangerous for mammalian cells as well [8, 33]. The polychromatic nature of plasma-generated UV radiation (see figure 2(a)) significantly limits the duration of plasma treatment in its application for wound disinfection. On the other hand, a relatively long irradiation time is required to achieve the concentrations of plasma-generated RS that are toxic for bacteria. The results of our study suggest that plasmas for wound disinfection should be optimized in the following ways: (i) intensity of plasma-generated UV radiation on the object should be reduced significantly, and (ii) densities of plasma-generated RS on the object should be increased in order to reduce the irradiation duration.

Acknowledgments

The plasma torch system used in this study was designed by B Steffes (MPE) and T Urayama (ADTEC Co. Ltd) and constructed by the ADTEC Co. Ltd, Japan. We thank Professor A Ullrich, Max-Plank Institute of Biochemistry, Germany, for his help with materials and equipment. We are also grateful to Professor W Stolz, Dr G Isbary, Clinic of Dermatology, Allergology and Environmental Medicine, and Dr H U Schmidt, Institute of Medical Microbiology, Munich-Schwabing, Germany, for useful discussions.

Appendix. Methods

A.1. Measuring UV, RS, pH, temperature and evaporation

The emission spectrum of the plasma-generated UV was measured using the AvaSpec-2048 Fiber Optic Spectrometer (Avantes, USA) at a distance of 16 mm from the plasma torch nozzle. During the measurements, the spectrometer detector faced the region of maximum light emission by plasma. To estimate the transmittance of the quartz glass used in our experiments, these measurements have been repeated with a quartz glass positioned in front of the spectrometer detector (see figure A.1). The UV light power density was measured in the 170–340 nm wavelength range using the Hamamatsu UV-Power Meter C8026 (Hamamatsu Photonics K.K., Japan). UV absorption by 2.5 mm layer of different liquids was measured using a 35/10 mm culture plate with a quartz glass bottom.

The concentration of NO_2 in the gas phase was measured using the Dräger X-am 7000 gas detector (Dräger Safety France S.A.S.). Since the sampled gas was pumped through a 20 cm long plastic tube (6.35 mm in diameter) at a flow rate of 200 sccm, the measurement is not precise in position (see figure 2(b)).

To assess the diffusion of RNS into liquids during plasma irradiation, we measured the concentration of nitrates and nitrites, final products of NO and NO_2 reactions in aqueous solutions. Nitrite and total nitrite/nitrate concentrations were determined using the Nitrate/Nitrite Fluorometric Assay Kit according to the manufacturer's protocol (Cayman Chemical, MI, USA; 780051). Fluorescence produced by reaction with nitrites was measured at 360 ± 20 nm excitation and 460 ± 20 nm emission wavelengths using the Synergy HT Multi-Mode Microplate Reader in conjunction with KC4 data reduction software (BioTek). Concentrations were calculated based on nitrite and nitrite/nitrate standard curves. Concentration of H_2O_2 in plasma-irradiated liquids was measured using Amplex Red Hydrogen

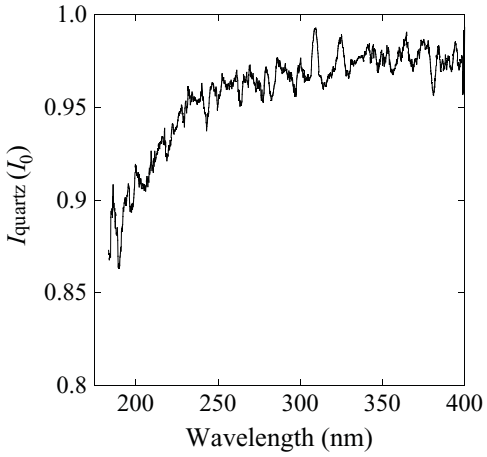

Figure A.1. Transmittance of the quartz glass in the UV range. Shown is the ratio of intensities of UV radiation produced by the torch with (I_{quartz}) and without (I_0) the quartz glass.

Peroxide/Peroxidase Assay Kit according to the manufacturer's protocol (Invitrogen, UK; A22188). Absorbance by hydrogen peroxide-containing samples ($\lambda = 570$ nm) was measured using ELISA microplate reader (BioTek). Concentrations were calculated based on the hydrogen peroxide standard curve.

The pH of plasma-irradiated liquids was measured using pH indicator strips that have a sensitivity of 0.5 (MercK KGaA, Germany). The temperature of liquids was measured using a small type-K thermocouple. Volumes of evaporated liquids were inferred from the volumes of liquids remaining in the well of the test plate after 1–10 min of plasma irradiation.

A.2. Assessing effects of plasma irradiation on bacteria

All experiments were performed using the XL1-Blue MRF′ *E. coli* strain (Stratagene; 200301). To quantitatively estimate bacterial density reduction after irradiation with plasma or plasma-generated UV, the *E. coli* suspension in LB medium or PBS (70 μl sample^{-1}) was irradiated in 96-microwell plates as described in section 2. Forty microliters of treated and untreated (control) samples were used to inoculate solid agar media in 100/15 mm Petri dishes either immediately after irradiation or after some period of incubation depending on the goal of the experiment (specified in section 3). To achieve bacterial density optimal for counting, samples that were incubated longer than one hour were 10× or 100× resuspended before plating. Cultures in Petri dishes were incubated at 37 °C overnight. Bacterial colonies in each Petri dish were counted manually.

To estimate the effect of plasma- or UV-generated RS on bacteria, 70 μl sample^{-1} of LB medium or PBS were irradiated in 96-microwell plates. Ten microliters from each irradiated and non-irradiated (control) sample were used for the analyses of nitrite/nitrate concentration (see appendix A.1). The remaining 60 μl were mixed with 10 μl of non-irradiated *E. coli* suspension either immediately after the liquid irradiation or after some period of incubation depending on the goal of the experiment. Samples inoculated with *E. coli* were incubated 60 min at room temperature and analyzed as described above.

To ensure the reproducibility of experimental results, each experiment was performed at least three times. In each experiment, samples were prepared and analyzed in duplicates.

A.3. Assessing effects of plasma-generated reactive species on human skin fibroblasts

A.3.1. Cell culture. The human foreskin fibroblast cell line hTERT-BJ1 was kindly provided by A Ullrich, Max-Plank Institute of Biochemistry (Germany). Cell cultures were maintained in the DMEM supplemented with 10% FCS, 25 μg ml^{-1} streptomycin, 25 μg ml^{-1} penicillin. The cells were grown in a humidified tissue culture incubator in 5% CO_2 at 37 °C.

A.3.2. Cell viability assay. To estimate the effect of plasma-generated RS (and products of their reactions) on hTERT-BJ1 viability, human skin fibroblasts were grown to 70% confluency in DMEM/10% FCS in 35/10 mm tissue culture plates (Greiner, Germany; 627160). For the cell necrosis assay, cell cultures were incubated in 1 ml of plasma-irradiated PBS or DMEM/0.1% FCS for 40 min and 4 h, respectively. To estimate the percentage of necrotic cells in treated and control samples, cells were trypsinized, stained with a vital dye trypan blue following the standard protocol (Freshney, 1987), and counted using hemocytometer.

For the cell apoptosis assay, cells were incubated in plasma-irradiated DMEM/10% for 72 h (the life cycle of hTERT-BJ1). Control samples were prepared similarly, except for plasma irradiation. After 72 h, cells were trypsinized and harvested by centrifugation. Quantification of apoptotic cells was performed using flow cytometry analysis as described in Riccardi and Nicoletti [34]. Briefly, cells were collected by centrifugation, resuspended in 500 μl PBS, and fixed with 4.5 mL of 70% ethanol. The fixed cells were washed with PBS, stained with the fluorescent propidium iodide (PI) and analyzed using the BD FACS Calibur (BD Biosciences). For each sample, 10 000 cells were acquired in a logarithmic mode. Percentage of apoptotic cells was calculated using the Cell Quest software (BD Biosciences).

A.3.3. Cell migration assay. *In vitro* scratch assay was carried out to assess the effect of plasma-irradiated medium on hTERT-BJ1 migration. Briefly, cells were grown to confluency in 35/10 mm tissue culture plates. A scratch was introduced using the tip of a 200 μl pipette. Scratch margins were marked at the outside bottom surface of the culture plates. Cultures were washed with PBS to remove detached cells and incubated in 1 ml of DMEM/0.1% FCS irradiated with plasma for 60 min. Control samples were prepared similarly except for plasma irradiation. Cultures were visualized and imaged using the Axio Observer A1 microscope (Zeiss). Scratch images were taken every 3 h until the complete scratch closure. Images were analyzed using the ImageJ software. Cells were counted in three different sectors (200 × 200 pixels) selected within the scratch region in treated and control samples.

To ensure the reproducibility of experimental results, each experiment was performed two times. In each experiment, samples were prepared and analyzed in duplicates.

References

[1] Fridman G, Friedman G, Gutsol A, Shekhter A B, Vasilets V N and Fridman A 2008 Applied plasma medicine *Plasma Process. Polym.* **5** 503–33

[2] Laroussi M 2008 The biomedical applications of plasma: a brief history of the development of a new field of research *IEEE Trans. Plasma Sci.* **36** 1612–4

[3] Fridman G, Peddinghaus M, Ayan H, Fridman A, Balasubramanian M, Gutsol A, Brooks A and Friedman G 2006 Blood coagulation and living tissue sterilization by floating-electrode dielectric barrier discharge in air *Plasma Chem. Plasma Process.* **26** 425–42

[4] Pompl R *et al* 2006 Efficiency and medical compatibility of low-temperature plasma sterilisation *6th Int. Conf. on Reactive Plasmas and 23rd Symp. on Plasma Processing: Proc. ICRP-6/SPP-23 (Sendai, Japan, January 2006)* pp 151–2

[5] Sladek R E J, Filoche S K, Sissons C H and Stoffels E 2007 Treatment of *Streptococcus mutans* biofilms with a nonthermal atmospheric plasma *Lett. Appl. Microbiol.* **45** 318–23

[6] Bloom D F, Cornhill J F, Malchesky P S, Richardson D M, Bolsen K A, Haire D M, Loop F D and Cosgrove D M III 1997 Technical and economic feasibility of reusing disposable perfusion cannulae *Biomed. Instrum. Technol.* **31** 248–9

[7] Rossi F, Kylián O and Hasiwa M 2006 Decontamination of surfaces by low pressure plasma discharges *Plasma Process. Polym.* **3** 431–42

[8] Horikawa-Miura M, Matsuda N, Yoshida M, Okumura Y, Mori T and Watanabe M 2007 The greater lethality of UVB radiation to cultured human cells is associated with the specific activation of a DNA damage-independent signaling pathway *Radiat. Res.* **167** 655–62

[9] Ohguro N, Fukuda M, Sasabe T and Tano Y 1999 Concentration dependent effects of hydrogen peroxide on lens epithelial cells *Br. J. Ophthalmol.* **83** 1064–8

[10] Scharffetter K, Wlaschek M, Hogg A, Bolsen K, Schothorst A, Goerz G, Krieg T and Plewig G 1991 UVA irradiation induces collagenase in human dermal fibroblasts *in vitro* and *in vivo Arch. Dermatol. Res.* **283** 506–11

[11] Waris G and Ahsan H 2006 Reactive oxygen species: role in the development of cancer and various chronic conditions *J. Carcinog.* **5** 14

[12] Shimizu T *et al* 2008 Characterization of microwave plasma torch for decontamination *Plasma Process. Polym.* **5** 577–82

[13] Rodeheaver G 2001 Wound cleansing, wound irrigation, wound disinfection *Chronic Wound Care: A Clinical Source Book For Healthcare Professionals* 3rd edn ed D Krasner, G Rodeheaver and R Sibbald (Malvern, PA: HMP Communications) pp 369–83

[14] Chau T T, Kao K C, Blank G and Madrid F 1996 Microwave plasmas for low-temperature dry sterilization *Biomaterials* **17** 1273–7

[15] Pollak J, Moisan M, Keroack D and Boudam M K 2008 Low-temperature low-damage sterilization based on UV radiation through plasma immersion *J. Phys. D: Appl. Phys.* **41** 135212

[16] Eguia J M and Chambers H F 2003 Community-acquired methicillin-resistant *Staphylococcus aureus*: epidemiology and potential virulence factors *Curr. Infect. Dis. Rep.* **5** 459–66

[17] Himmelblau D M 1964 Diffusion of dissolved gases in liquids *Chem. Rev.* **64** 527–50

[18] Zacharia I G and Deen W M 2005 Diffusivity and solubility of nitric oxide in water and saline *Ann. Biomed. Eng.* **33** 214–22

[19] Imlay J A and Linn S 1986 Bimodal pattern of killing of DNA-repair-defective or anoxically grown *Escherichia coli* by hydrogen peroxide *J. Bacteriol.* **166** 519–27

[20] Pacelli R, Wink D A, Cook J A, Krishna M C, DeGraff W, Friedman N, Tsokos M, Samuni A and Mitchell J B 1995 Nitric oxide potentiates hydrogen peroxide-induced killing of *Escherichia coli J. Exp. Med.* **182** 1469–79

[21] Allaker R P, Silva Mendez L S, Hardie J M and Benjamin N 2001 Antimicrobial effect of acidified nitrite on periodontal bacteria *Oral Microbiol. Immunol.* **16** 253–6

[22] Woodmansee A N and Imlay J A 2003 A mechanism by which nitric oxide accelerates the rate of oxidative DNA damage in *Escherichia coli*. *Mol. Microbiol.* **49** 11–22

[23] Luo Y, Han Z, Chin S M and Linn S 1994 Three chemically distinct types of oxidants formed by iron-mediated Fenton reactions in the presence of DNA *Proc. Natl. Acad. Sci. USA* **91** 12438–42

[24] Farias-Eisner R, Chaudhuri G, Aeberhard E and Fukuto J M 1996 The chemistry and tumoricidal activity of nitric oxide/hydrogen peroxide and the implications to cell resistance/susceptibility *J. Biol. Chem.* **271** 6144–51

[25] Nathan C F 1987 Secretory products of macrophages *J. Clin. Invest.* **79** 319–26

[26] MacMicking J, Xie Q W and Nathan C 1997 Nitric oxide and macrophage function *Annu. Rev. Immunol.* **15** 323–50

[27] Yoshioka Y, Kitao T, Kishino T, Yamamuro A and Maeda S 2006 Nitric oxide protects macrophages from hydrogen peroxide-induced apoptosis by inducing the formation of catalase *J. Immunol.* **176** 4675–81

[28] Wink D A, Hanbauer I, Krishna M C, DeGraff W, Gamson J and Mitchell J B 1993 Nitric oxide protects against cellular damage and cytotoxicity from reactive oxygen species *Proc. Natl. Acad. Sci. USA* **90** 9813–7

[29] Kotamraju S, Tampo Y, Keszler A, Chitambar C R, Joseph J, Haas A L and Kalyanaraman B 2003 Nitric oxide inhibits H_2O_2-induced transferrin receptor-dependent apoptosis in endothelial cells: role of ubiquitin–proteasome pathway *Proc. Natl. Acad. Sci. USA* **100** 10653–8

[30] Chae H J, Kim H R, Kwak Y G, Ko J K, Joo C U and Chae S W 2001 Signal transduction of nitric oxide donor-induced protection in hydrogen peroxide-mediated apoptosis in H9C2 cardiomyoblasts *Immunopharmacol. Immunotoxicol.* **23** 187–204

[31] Gray D, Kilkson R and Deering R A 1965 Inactivation of oriented bacteria with polarized ultraviolet light *Biophys. J.* **5** 473–86

[32] Pollak J, Moisan M, Keroack D and Boudam M K 2008 Low-temperature low-damage sterilization based on UV radiation through plasma immersion *J. Phys. D: Appl. Phys.* **41** 135212

[33] Koch-Paiz C A, Amundson S A, Bittner M L, Meltzer P S and Fornace A J Jr 2004 Functional genomics of UV radiation responses in human cells *Mutat. Res.* **549** 65–78

[34] Riccardi C and Nicoletti I 2006 Analysis of apoptosis by propidium iodide staining and flow cytometry *Nat. Protoc.* **1** 1458–61